9.6 TESTS OF A SATELLITE-BASED CLOUD INITIALIZATION SCHEME FOR HIGH LATITUDE APPLICATION IN MM5

Xingang Fan* and Jeffrey S. Tilley
Geophysical Institute, University of Alaska Fairbanks, Fairbanks, AK 99775

1. INTRODUCTION

A continuing problem with respect to regional weather and climate model simulations relates to the fact that the standard versions of many mesoscale models are not set up to provide for a proper initialization of cloud hydrometeor fields (e.g., cloud water, ice and snow mixing ratios, and rain water) Thus, the model has to spend time to spin-up these variables, and their associated cloud systems and latent heating, from other initial fields during the first few (0-6) hours of simulation. Adjustments that occur to the other model fields through this spin-up process can result in a gradual drift of the model simulation away from the actual conditions and lead to a degraded forecast. Moreover, due to the complex nonlinearity of atmospheric models, initial errors can grow exponentially with time (Lorenz, 1963). Therefore, shortening the spin-up period should benefit the forecasts. Also, if the model initial state were to contain clouds (via associated hydrometeor mixing ratio fields), the model initial state would be closer to that of the real atmosphere and the spin-up process could be largely avoided, leading to improved simulations within the first few hour and thereafter.

The Penn State University (PSU)/National Center for Atmospheric Research (NCAR) mesoscale modeling system (MM5) is used all over the world for research and operational mesoscale weather simulation and forecasts. (Dudhia, 1989; Grell et al, 1994; Chen and Dudhia, 2001). The model contains physical schemes for both convective and large scale clouds. Convective parameterization represents subgrid-scale transports by updrafts and downdrafts, which vertically redistribute heat, moisture, and momentum within model resolved columns and also produce convective clouds and rainfall. Explicit microphysical schemes act to reproduce stratiform clouds and their associated latent heating and precipitation.

The purpose of this study is to attempt to minimize model spin-up by initiating model clouds at the forecast initial time. The model will then start integration with cloud hydrometeors available from the beginning. A static initialization scheme has been put forward in this paper to initialize model clouds based on a given atmospheric status. The procedure to accomplish the above objectives reproduces the large scale clouds via an explicit moisture scheme, specifically the MM5 Reisner mixed-phase scheme (Reisner et al, 1998). Details of the procedures and utilization of the scheme for cloud initialization are discussed.

In addition to the cloud initialization, accurate moisture profiles are another crucial requirement in terms of forecasting, since accurate clouds can be obtained only when there is an accurate moisture distribution. Fan and Tilley (2002) assimilated Advanced Very High Resolution Radiation (AVHRR) data from NOAA satellites into MM5 analysis to adjust the model moisture fields so that the model could produce more accurate clouds. Their results, obtained for a high-latitude heavy rain case where cloud top brightness temperatures are assimilated, showed that satellite observations often provide adequate information to benefit cloud forecasts. Continuous or near-continuous assimilation, such as the intermittent approach in Fan and Tilley (2002), of satellite data improved the simulation for a longer time range.

However, only the brightness temperature of AVHRR channel 4 was used in Fan and Tilley (2002). Better satellite data sources are available now, such as the Moderate Resolution Imaging Spectroradiometer (MODIS) instruments onboard the NASA satellites Terra and Aqua. MODIS atmospheric level-2 products provide retrievals of water vapor and cloud properties, as well as the temperature and dew point temperature profiles. Such products are used in this study for determining the clouds and retrieving moisture profiles.

In the procedure to incorporate MODIS data,

* *Corresponding Author Address*: Dr. Xingang Fan, University of Alaska Fairbanks, Geophysical Institute, Fairbanks, AK 99709.
Email: ffxf@uaf.edu

the vertical profiles of temperature and dew point temperature, and cloud top properties have been derived from MODIS products and utilized in the previously developed cloud initialization scheme. The scheme also takes advantage of the MM5 analysis in the determination of initial model humidity fields in cloudy areas.

The cloud initialization scheme has been tested for a period during mid-August 2001 characterized by substantial clouds and precipitation over western Alaska and the southern slopes of the Brooks Range stemming from a series of short wave disturbances within a rapid westerly mid-tropospheric flow pattern. Numerical experiments utilizing the cloud initialization scheme and MODIS data during this period are performed. Results from these initial tests and a preliminary evaluation of the scheme performance are presented in this paper.

2. SYNOPTIC CASE AND MODEL CONFIGURATION

2.1 Case Study

Figure 1 shows the NCAR/National Centers for Environmental Prediction (NCEP) reanalysis weather patterns and cloud cover during the case under consideration, 13-16 August 2001. This period was characterized by considerable cloudiness and precipitation. 4-day averaged geopotential heights at 850 hPa valid for the 13-16 August period (Figure 1a) depict a propagating westerly flow pattern in the mid-troposphere. This flow pattern is sustained via the presence of a deep low in the western Arctic Ocean and a ridge south of the Alaska Peninsula. Another low is also present in the northeast Pacific Ocean. Through the westerly flow pattern, a series of short wave disturbances propagated west to east, causing substantial clouds and precipitation over western Alaska and the southern slopes of the Brooks Range. The 1440 m contour lines for every 12 hours between 12UTC 13 August and 12UTC 16 August are also shown on Figure 1a. These contours clearly illustrate the short waves during the period. Figure 1b shows the 4-day average of total cloud coverage; the cloud coverage pattern reinforces the necessity of performing cloud initialization for model runs for any time during this period.

The precipitation during this period reflects the fast-moving short wave disturbances. Figure 2 shows the observed 1-hour precipitation in the MM5 domain, from 01 to 04UTC, August 14, 2001, for the purpose of verifying the cloud initialization scheme.

2.1 Model Configuration

The MM5 model is setup to run on a domain with 45-km grid spacing, centered at 60.6°N latitude and 150°W longitude. Forty-one sigma levels are used in the vertical. The standard MM5 model accommodates four-dimensional data assimilation (FDDA) via Newtonian nudging. The model also contains various physical parameterizations. All the simulations in this study use the Grell cumulus parameterization (Grell, 1994) and the Reisner et al (1998) explicit moisture scheme without graupel. The Oregon State University (OSU) land surface model (LSM, Chen and Dudhia, 2001), Hong and Pan (1996) planetary boundary layer (PBL) scheme, and Dudhia (1989) 2-stream radiative transfer are also

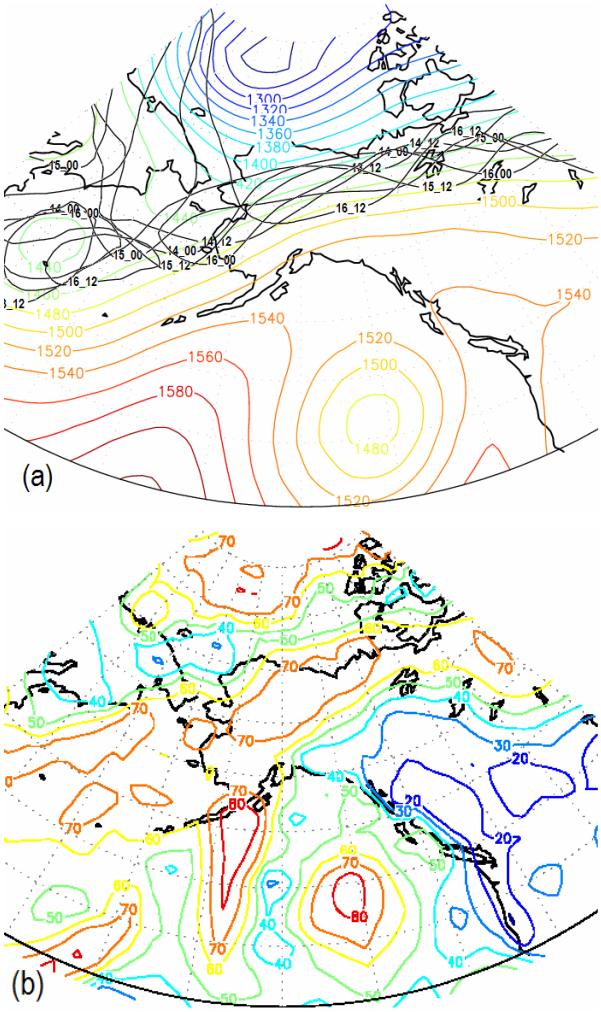

Figure 1. Mean 850 hPa geopotential height (m, a) and mean total cloud cover (%, b), averaged over Aug. 13, 2001 to Aug. 16, 2001. The imposed black colored contours with date and hour labels (dd_hh) in panel (a) are 850 hPa height of 1440 m at the labeled time.

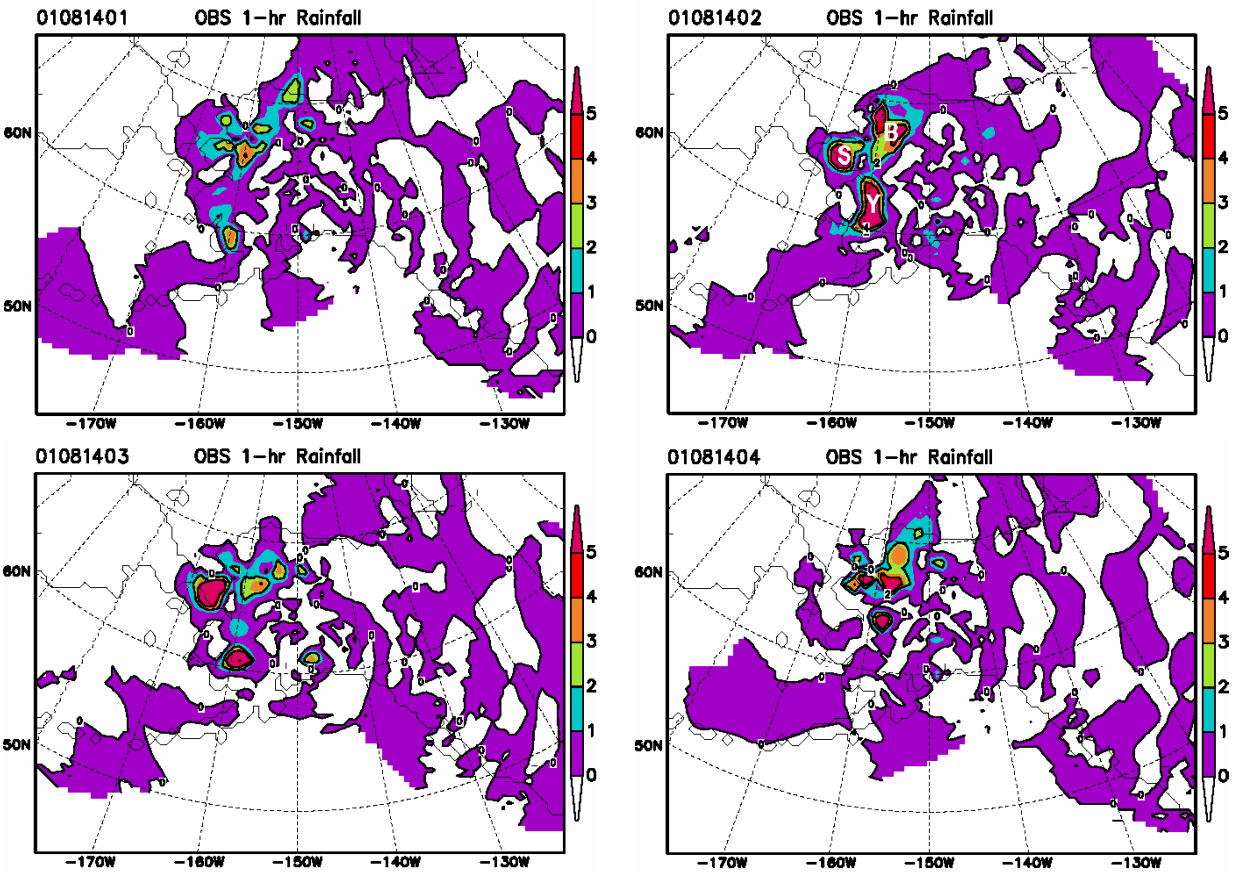

Figure 2. Station observed 1-hour rainfall (mm) from 01 to 04 UTC August 14, 2001.

used. Initial atmospheric conditions are obtained from the NCAR/NCEP reanalysis, and are enhanced by surface and upper air observations through objective analysis.

The initial time point for testing the static cloud initialization scheme is set to 00UTC August 14, 2001, which is cited as hour zero in the experiments. The simulations run from either hour -6 or 0 through hour 12, with a time step of 2 minutes.

3. CLOUD INITIALIZATION SCHEME

While there are always large areas that are covered by clouds, the standard MM5 model has not been set up to contain clouds explicitly at the initial time. So, initial clouds need to be determined from the observed and/or analyzed temperature and humidity environment.

The mixed phase processes contained within the MM5 Reisner1 scheme (Reisner et al, 1998) are used here for cloud initialization. For the purpose of a static initialization, production of rain at the initial time is omitted from the diagnostic equations of water vapor, cloud water and cloud ice, since the fallouts would carry the cloud hydrometeors to lower levels. In other words, no precipitation processes are included. Processes included are cloud processes, including: (1) ice crystal initiation, (2) deposition on to ice crystals, and (3) condensation /evaporation of cloud hydrometeors. These processes for ice and cloud are shown in the box diagram in Figure 3. On the basis of the above assumptions, the equations associated with the moist processes are:

$$\frac{\partial}{\partial t} p^* T = \frac{p^* Q}{c_p} \tag{1}$$

$$\frac{\partial}{\partial t} p^* q_v = p^* \left(- PRI - PRD - PCON \right) \tag{2}$$

$$\frac{\partial}{\partial t} p^* q_c = p^* \left(PRI + PRD + PCON \right) \tag{3}$$

where the terms PRI, PRD, and PCON stand for

ice crystal initiation, deposition on to ice crystals, and condensation/evaporation of cloud, respectively, as adopted from Dudhia (1989) and Reisner et al (1998). All other variables in the equations (1) – (4) except p^* follow standard conventions and are same as those in Hsie et al (1984). p^* is defined as the difference between surface pressure (p_s) and model top pressure (p_t):

$$p^* = p_s - p_t \tag{4}$$

The latent heating due to the moist processes is:

$$Q = L(PRI + PRD + PCON) \tag{5}$$

The scheme is implemented at the initial time (i.e., forecast hour zero). Given enough iteration steps (or time) to run the above initialization scheme, the model cloud water, ice and water vapor will reach a state of equilibrium. Then, the model run can be resumed with the hydrometeors as determined at the end of the iteration procedure.

Figure 4 shows the results of a single column at grid point (41, 34) when utilizing the scheme. The scheme was iterated for 180 time steps, equivalent to a 6-hour period. The total change of temperature (T), water vapor (Qv), cloud water (Qc), and cloud ice (Qi) versus iteration time steps at each sigma level are shown in Figure 4. It can be concluded that the ice, water and vapor almost

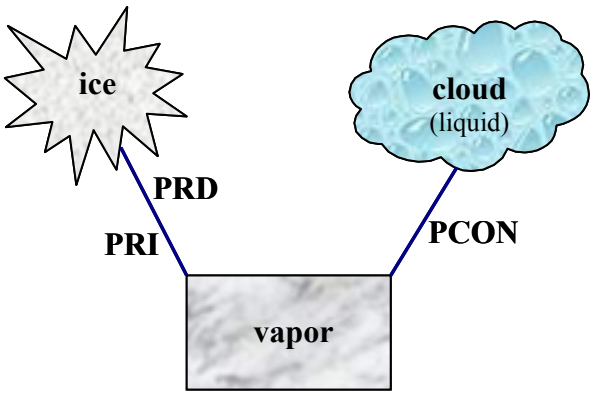

Figure 3. Processes in the moisture scheme for ice (crystals), cloud (liquid) and water vapor. PRI, initiation of ice crystals; PRD, deposition on to ice crystals; and PCON, condensation/evaporation of cloud.

Figure 4 shows the results of a single column at grid point (41,34) when performing the cloud initialization. The scheme was iterated for 180 time steps, equivalent to a 6-hour period. The total change of temperature (T), water vapor (Qv), cloud water (Qc), and cloud ice (Qi) versus iteration time steps at each sigma level are shown in Figure 4. It can be concluded that the ice, water

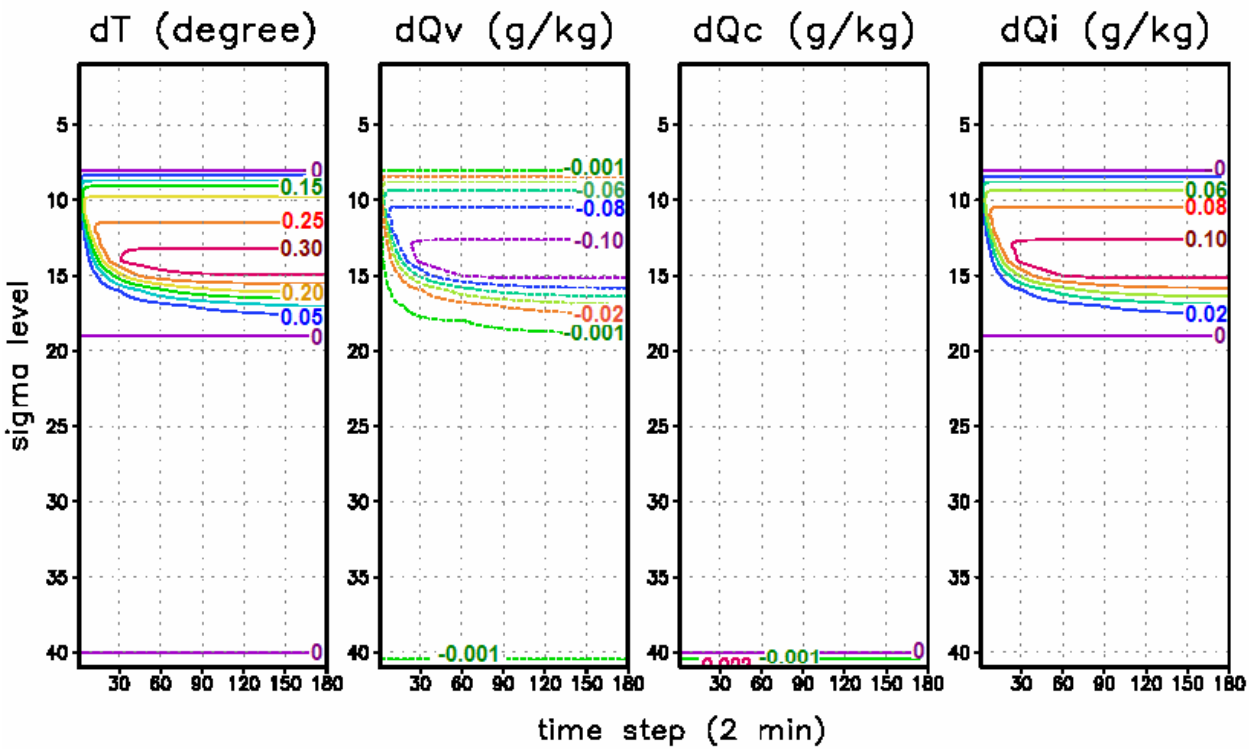

Figure 4. The total change of temperature (dT), water vapor (dQv), cloud water (dQc), and cloud ice (dQi) versus time at each sigma level of the column at grid point (41,34).

and vapor almost reaches an equilibrium state about 3 hours for this column. The results of other columns are similar, which indicate that the scheme reproduces some cloud structure for the initial time. However, this scheme is only a static initialization. There are other mechanisms in the moving atmosphere that affect the initial clouds, including advection, convection, and precipitation processes.

4. DERIVATION OF HUMIDITY FROM MODIS

The success of the cloud initialization also depends on the accuracy of the initial water vapor content. A more realistic humidity field such as could be derived from observations, could advance the cloud initialization and allow for a faster convergence of the scheme. MODIS level 2 data can provide retrieved atmosphere moisture (dew point temperature) profiles and temperature profiles in cloud-free areas. The MODIS data has 1-km resolution and 20 vertical pressure levels. After interpolated to 41 vertical levels and to the MM5 45-km grid resolution, this data can be incorporated directly where it is clear.

For cloudy areas, MODIS can provide information on cloud top temperature and cloud top pressure. By using these data, a more accurate model cloud top can be found than only using one kind of data such as cloud top brightness temperature. Cloud base is determined following the method used in Fan and Tilley (2002). Once cloud top and base are determined, the humidity profile in the cloudy column can be ascertained by using the MM5 analysis together with a set of empirically derived relative humidity thresholds (Table 1; from Fan and Tilley 2002). The relative humidity thresholds, for clear and cloudy areas, are denoted by *RHcld* and *RHclr*, respectively. In the scheme, the relative humidity is set greater than *RHcld* where there is cloud and less than *RHclr* where it is clear. Fan and Tilley (2002) have shown that the MM5 can produce more realistic cloud cover when the adjusted humidity fields are used. In this paper, both the MM5 analyzed humidity profile and the relative humidity thresholds are used in order that a humidity structure similar to the MM5 analysis is obtained while the adjusted humidity fields can potentially produce more realistic cloud fields.

4.1 Cloud Top and Base

As for all remotely-sensed fields, the MODIS retrieved products contain errors. Specifically, the maximum error for cloud top pressure (denoted by *CTPerr*) is 100 hPa, and the maximum error for temperature profiles (denoted by *CTTerr*) is about 2 K (MTBD MODIS). As mentioned above, the MM5 analysis can also suggest clouds by utilizing the relative humidity thresholds in Table 1. Therefore, the cloud top is determined by using all three sources of information.

Table 1 *RH* (%) thresholds at different sigma levels for both cloud and clear conditions.

Level # (σ)	RH_{cld}	RH_{clr}	Level # (σ)	RH_{cld}	RH_{clr}
1 (0.0090)	85.0	55.0	**22** (0.6065)	94.4	77.0
2 (0.0290)	85.5	56.1	**23** (0.6385)	94.7	77.9
3 (0.0500)	86.0	57.2	**24** (0.6705)	95.0	78.8
4 (0.0725)	86.5	58.3	**25** (0.7025)	95.3	79.7
5 (0.0960)	87.0	59.4	**26** (0.7335)	95.6	80.6
6 (0.1205)	87.5	60.5	**27** (0.7635)	95.9	81.5
7 (0.1460)	88.0	61.6	**28** (0.7920)	96.2	82.4
8 (0.1725)	88.5	62.7	**29** (0.8190)	96.5	83.3
9 (0.2000)	89.0	63.8	**30** (0.8435)	96.8	84.2
10 (0.2285)	89.5	64.9	**31** (0.8665)	97.0	85.0
11 (0.2580)	90.0	66.0	**32** (0.8875)	97.2	85.8
12 (0.2880)	90.5	67.1	**33** (0.9070)	97.4	86.6
13 (0.3190)	91.0	68.2	**34** (0.9245)	97.6	87.4
14 (0.3505)	91.4	69.2	**35** (0.9405)	97.8	88.2
15 (0.3825)	91.8	70.2	**36** (0.9550)	98.0	89.0
16 (0.4145)	92.2	71.2	**37** (0.9680)	97.5	89.1
17 (0.4465)	92.6	72.2	**38** (0.9790)	97.0	89.2
18 (0.4785)	93.0	73.2	**39** (0.9875)	96.5	89.3
19 (0.5105)	93.4	74.2	**40** (0.9935)	96.0	89.4
20 (0.5425)	93.8	75.2	**41** (0.9975)	95.0	89.0
21 (0.5745)	94.1	76.1			

If the cloud top level suggested by the MM5 analysis is within the range of *CTP*±*CTPerr* or *CTT*±*CTTerr*, the MM5 cloud top is retained. Otherwise, the cloud top level will be determined by matching the MODIS cloud top pressure and temperature with the MM5 analysis. Assume the cloud top level is found at *Kp* and *Kt* by pressure and temperature, respectively. If *Kp* and *Kt* are close enough that *P*(*Kp*) ±*CTPerr* and *T*(*Kt*) ±*CTTerr* overlap along the vertical sigma level, the mid sigma level *Km* between *Kp* and *Kt* is determined as the cloud top level, when error ratios to both *CTPerr* and *CTTerr* are approximately equal:

$$\frac{|P(Km)-P(Kp)|}{CTPerr} \approx \frac{|T(Km)-T(Kt)|}{CTTerr}. \qquad (6)$$

If *Kp* and *Kt* are far apart, assuming the level *Kp* is above (or below) the level *Kt*, a mid sigma level between levels where *P*=*P*(*Kp*)+*CTPerr* (or *P*=*P*(*Kp*)-*CTPerr*) and *T*=*T*(*Kt*)-*CTTerr* (or *T*=*T*(*Kt*)+

CTTerr) is chosen as the cloud top level.

Determination of cloud base follows the procedure in Fan and Tilley (2002). However, the criteria Fan and Tilley (2002) used for the difference of cloud base temperature from surface temperature and maximum column temperature has been found to be large at some grid points. After examining several ocean and land grid points, the criteria have been changed to 2.0 and 2.5 K for ocean grid points and 2.5 and 3.0 K for land grid points. This is partly due to the fact that temperature inversions often exist over the high-latitude regions as pointed out by Fan and Tilley (2002).

Let the model analyzed surface temperature be denoted by T_g and the maximum temperature within the vertical volume by T_m. For ocean grid points, the cloud base is at the level where the temperature equals the larger of (T_g-2.0) and (T_m-2.5). For land grid points, the cloud base is at the level where the temperature equals the larger of (T_g-2.5) and (T_m-3.0). In order to avoid the impacts of inversions at lower levels, the second layer from the surface where the temperature satisfies the above condition(s) is identified as cloud base when more than one inversion exists (Fan and Tilley, 2002).

4.2 Humidity

MODIS-retrieved relative humidity, computed from the MODIS temperature and dew point temperature fields, is used where it is available. Unlike within a large cloudy area, some small cloudy areas surrounded by clear points may also have MODIS-retrieved humidity which is a good source of information and is used anyway.

The humidity for cloudy grid points is adjusted by utilizing both the previously obtained cloud distribution and relative humidity thresholds as well as referencing the MM5 analyzed humidity profile. For levels above the cloud top level, if any relative humidity is not greater than the *RHclr* of any level, MM5 analyzed humidity is left unchanged. Otherwise, we first find the level that has the maximum positive difference of relative humidity from its *RHclr*. Then, the ratio of the maximum difference to the difference of (*RHcld*-*RHclr*) is calculated. Then, half of this ratio is applied to compute, from each level's (*RHcld*-*RHclr*), the amount to adjust that level's relative humidity.

Due to the approximate nature of the method used to obtain the cloud base, the MM5 analyzed humidity below the cloud base level is left unchanged.

For the levels between cloud top and cloud base, the humidity is adjusted according to the MM5 analysis at the cloud top level. If the relative humidity at the cloud top level is greater or equal to *RHcld*, no adjustment is needed. Otherwise, the ratio of the difference between cloud top level relative humidity and its *RHcld*, to the difference between *RHcld* and *RHclr* is calculated. Then the same ratio is applied to all the levels below cloud top to calculate the amount of adjustment from each level's (*RHcld*-*RHclr*).

The water vapor mixing ratio (q) is used in the standard MM5 initial conditions. Therefore, all above adjusted relative humidities are then converted to q for use in the MM5.

5. EXPERIMENTS AND RESULTS

5.1 Experiment Design

Preliminary tests for the cloud initialization scheme are performed via a series of experiments listed in Table 2.

Experiment C-6h is used as a baseline experiment, in which the FDDA option for Newtonian nudging was turned on during the first 6 hours and the model is continuously run through the experiment hour 0, 00UTC Aug. 14, 2001. The simulated model state will, at least theoretically, be closer to the analysis at the hour 0, the time that the other experiments start. Thus, the effective spin-up of the other four experiments can be shown clearly by comparing with the baseline experiment.

Experiment C0h is the standard MM5 starting from hour 0 without FDDA. The cloud initialization scheme is tested with the standard MM5 in experiment C0hci. The experiments C0hmodis and C0hcimodis are similar to C0h and C0hci except the MODIS data is assimilated.

The MODIS data is assimilated only at the initial time because the main purpose of this study

Table 2 Experiment design

Experiment	Description		
	Start and end hour†	Cloud initialize	MODIS data
C-6h‡	-6, 12	no	No
C0h	0, 12	no	No
C0hci	0, 12	yes	No
C0hmodis	0, 12	no	Yes
C0hcimodis	0, 12	yes	Yes
Notes	† Analysis nudging was used from -6 to 0 hour.		
	‡ hour 0 is at 00UTC August 14, 2001		

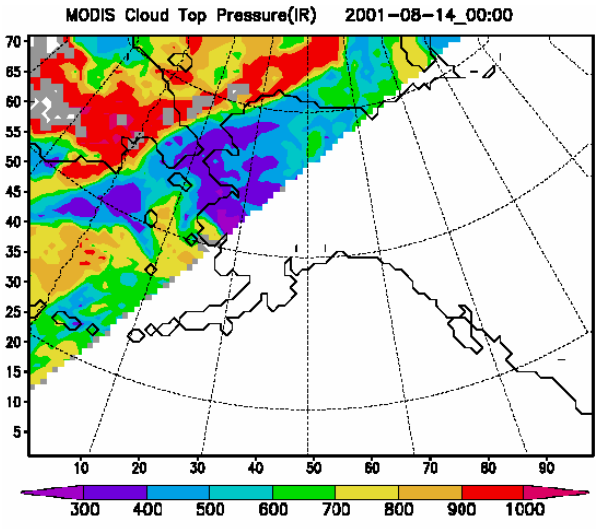

Figure 5. MODIS retrieved cloud top pressure from infrared channels at 00UTC August 14, 2001 (gray color means missing data).

is focused on initial conditions. The coverage of MODIS data at the initial time, 00UTC August 14, 2001, is shown in Figure 5, where only the cloud top pressure from infrared channels is illustrated as an example. In fact, the MODIS data at this time comprises four granules observed within 20 minutes around 00UTC, a reasonable period of time to be used for the 00UTC model initial time. The spatial coverage of the MODIS granules adequately covers our area of interest.

5.2 Verification

In order to verify the MM5 precipitation, bias and equitable threat (ETS) scores are calculated based on a contingency table approach (Wilks, 1995; Colle, 1999). The contingency table is shown in Figure 6. It is a 2x2 matrix, where each element of the matrix holds the number of occurrences in which the model and the observations did or did not reach a certain threshold amount. Based on the contingency table, a bias score is defined as

$$Bias = \frac{F}{O} = \frac{A+B}{A+C}, \tag{7}$$

where F is the number of forecasts at the observation stations with precipitation equal or exceeding a given threshold and O if the number of occurrences in which the observations meet or exceed the threshold. Thus, the bias score indicates how well the model predicted the frequency of occurrence of a given threshold, although it provides no information on the accuracy of forecasts. The ETS measures the skill in predicting a given threshold at a location and is defined by

$$ETS = \frac{H-E}{F+O-H-E} = \frac{A-E}{A+B+C-E}. \tag{8}$$

Here H is the number of forecast "hits", where both the model and observation point meet or exceed a given precipitation threshold, F and O are defined above, and E is defined as

$$E = \frac{F \cdot O}{N} = \frac{(A+B)(A+C)}{N}, \tag{9}$$

where N is the total number of observations verified (Mesinger, 1996).

The bias and ETS scores defined in (7) and (8) only measure model accuracy based on the frequency of occurrence at or above a threshold, and thus do not measures the magnitude of the precipitation forecast error. To examine the error magnitudes, the root-mean-square errors (RMSE) between the experiments are also calculated for other atmospheric variables by:

$$RMSE = \sqrt{\frac{1}{N}\sum_{i=1}^{N}\left(X_i - X_i^o\right)^2} \tag{10}$$

For a given Threshold		**Observation**	
		Yes	No
Model	Yes	A	B
	No	C	D

Figure 6. Contingency table, where A, B, C and D holds the number of occurrences in which the model and the observations did (Yes) or did not (No) reach or exceed a given threshold.

5.3 Results

a) *Modeled precipitation*

Figure 7 shows the simulated 1-hourly accumulated precipitation from experiments C-6h, C0h, and C0hcimodis, for forecast hours 1-3. Obviously, the continuous simulation in C-6h captured precipitation during the first hour, while experiments C0h and C0hcimodis only produced a tiny amount of rain. The MODIS data assimilation and cloud initialization made the experiment C0hcimodis produced two small rain

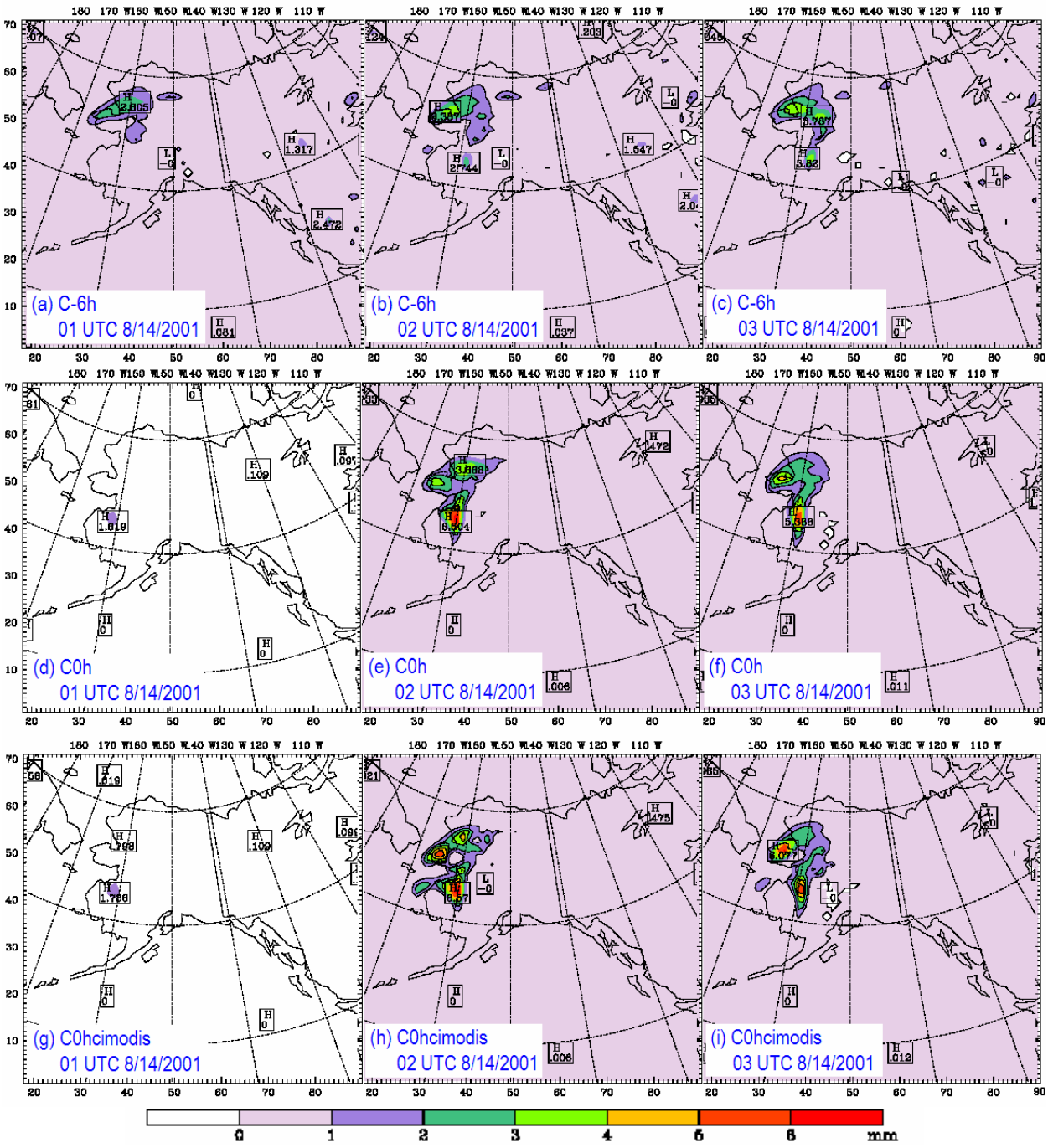

Figure 7. Simulated 1-hour accumulated total precipitation (mm) from experiments C-6h, C0h, and C0hcimodis, valid at 01, 02, and 03 UTC August 2001.

areas in the western Alaska and slightly more than the control run C0h. In the second hour, the observed rainfall has three major centers, one in the southwest of the Brooks Range (B on Figure 2b), one on Seward Peninsula (S on Figure 2b), and one in the lower Yukon Valley (Y on Figure 2b). Experiment C-6h under-forecasted the Yukon Valley rain center and produced a larger rain area included both the B and S areas. The control run, C0h, captured the rain center Y, as did experiment C0hcimodis. Starting from hour 2, experiments C0h and C0hcimodis performed better than experiment C-6h. This implies that the continuous run has lost some information from its initial conditions and has drifted from the analyzed status of the hour zero, the initial time point of

experiments C0h and C0hcimodis, despite FDDA being turned on. Perhaps stronger FDDA constraints (i.e., larger nudging coefficients) could improve it for this case.

The impact of MODIS data assimilated at the initial time can be read from Figure 7h that shows sufficient precipitation and a clearer pattern with all the three rain centers than in Figure 7e. The precipitation distribution simulated in experiments C0hcimodis (Figure 7h and 7i of hour 2 and hour 3, respectively) contains more details than that of C0h in comparing to the observations. The precipitation forecasts from experiments C0hci and C0hmodis (not shown) show little difference from C0h and C0hcimodis, respectively.

In order to quantitatively verify the precipitation simulations with observations, the equitable threat score (ETS) and bias are calculated using the definitions of (7)-(9). Because gridded rainfall observations may introduce noise (Figure 2), the ETS and bias are calculated relative to station observations. Accordingly, the model forecast of the closest grid point to a station is used as the model results for the station. Figures 8 and 9 show the ETS and bias, respectively, for four precipitation thresholds, 0.2, 1, 2, and 4 mm.

During the first hour, Figures 8 and 9 show that the baseline experiment C-6h captures most of the rainfall at the thresholds 0.2, 1, and 2 mm. The control run C0h has the lowest ETS for all the thresholds, while there is an increase in ETS for the 0.2 mm threshold going from experiment C0hci, C0hmodis to C0hcimodis. The bias scores for the 0.2 mm threshold increase toward 1 (a perfect forecast) going from experiments C0h, C0hmodis, to C0hcimodis. These results suggest positive effects of the cloud initialization scheme and the assimilation of MODIS data.

For forecast hour 2, the control run C0h did the best for the 0.2 and 2 mm thresholds, but experiment C0hcimodis has the highest skill for a 1 mm rainfall forecast as well as a bias score nearly equal to 1.

For forecast hour 3, experiment C0hcimodis shows high skill and closer to 1 bias scores at the 1 and 2 mm rainfall thresholds comparing to experiment C0h. Experiment C0h has high ETS for the 0.2 mm rainfall threshold, but the corresponding bias score suggests that it overdone more than C0hcimodis. In all the experiments and observations as well, there were

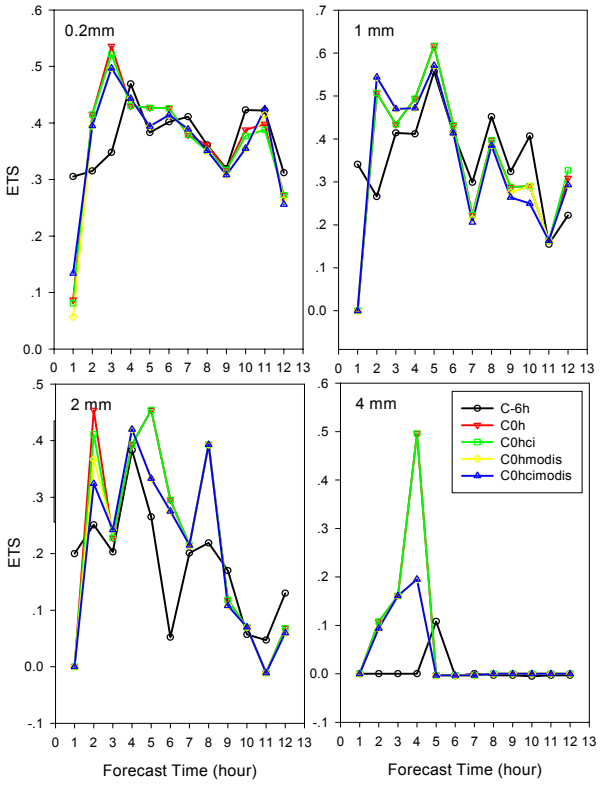

Figure 8. Equitable threat scores of simulated and station observed precipitation at thresholds of 0.2, 1, 2, and 4 mm

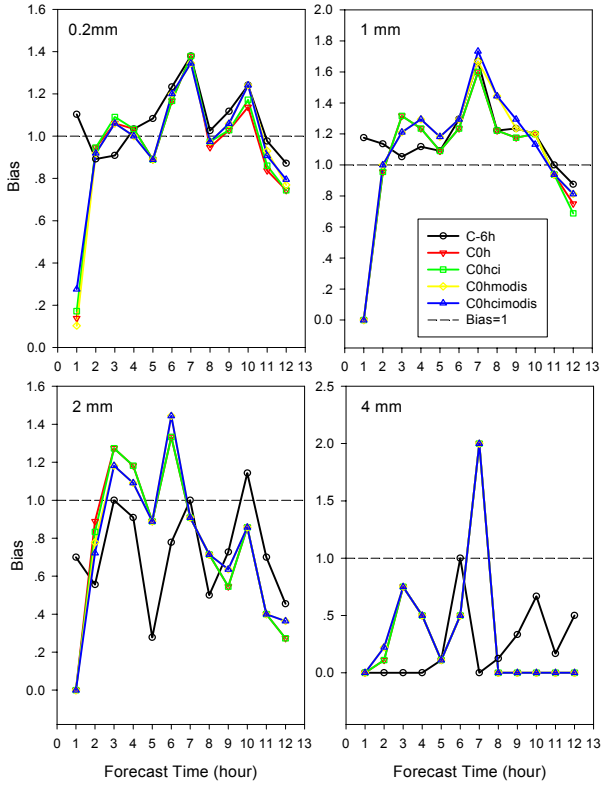

Figure 9. Bias scores of simulated and station observed precipitation at thresholds of 0.2, 1, 2, and 4 mm

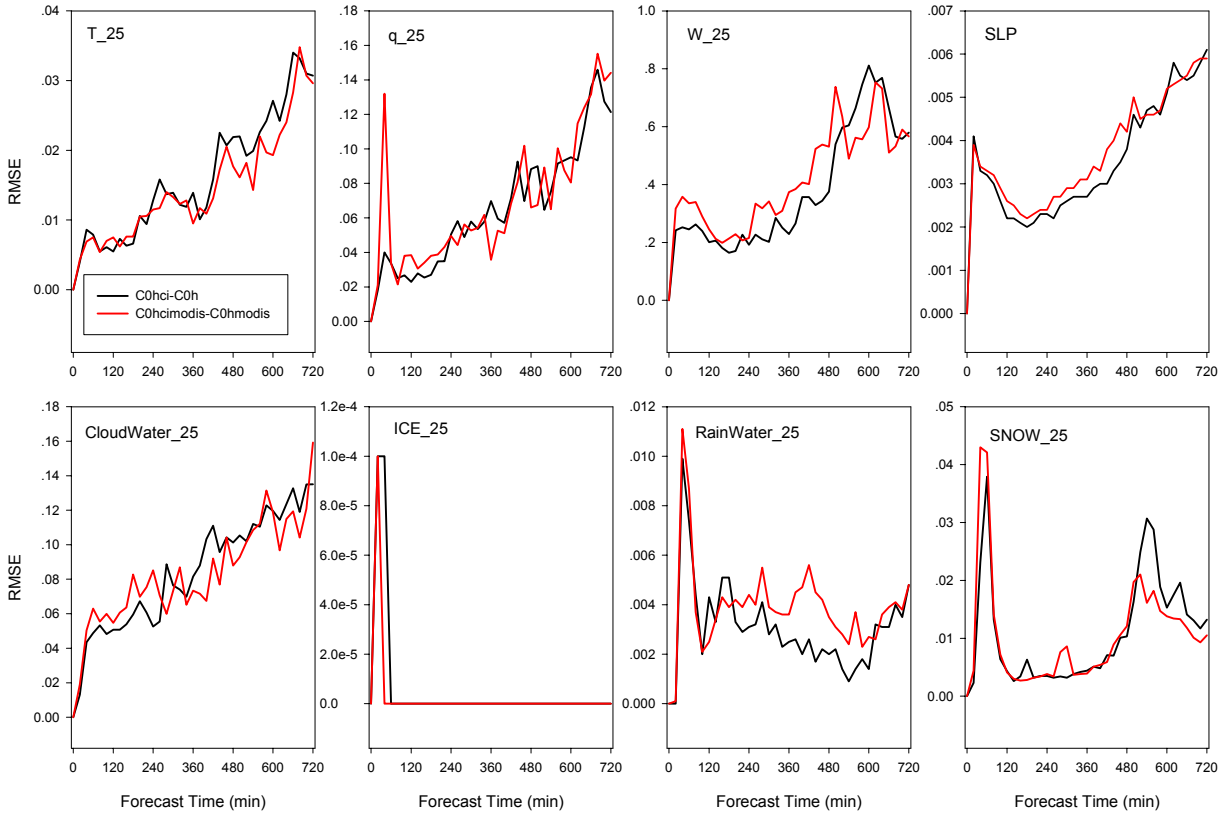

Figure 10. Root mean square error between experiments C0hci and C0h, C0hcimodis and C0hmodis. 25 indicates the 25th sigma level; T for temperature (K); q for water vapor mixing ratio (0.1g/Kg); W for vertical velocity (mm/s); SLP for sea level pressure (hPa); The cloud water, cloud ice, rain water, and snow are all in 0.1g/Kg.

few occurrences of 4 mm and above rainfalls. The figures only show some skill during the time period of hour 1-4.

A result related to the spin-up problem can also be obtained from Figures 8 and 9. All the experiments started from hour 0 have higher ETS and lower biases than the baseline experiment C-6h in most cases within the first 6 hours. This shows further the spin-up period in terms of precipitation.

Although the precipitation forecasts benefit from the cloud initialization and MODIS data, the differences between C0hci and C0h, C0hcimodis and C0hmodis have not been clearly shown. More forecast variables need to be analyzed to verify the impacts of the cloud initialization. We present some of these results in the next subsection.

b) *Modeled cloud hydrometeors and atmospheric states*

The root mean square errors (RMSE) have been calculated between the experiments. Figure10 shows RMSE of temperature (*T*), water vapor mixing ratio (*q*), vertical velocity (*W*), cloud water, cloud ice, rain water, and snow on the 25th sigma level, where most cloudy areas show the impacts from cloud initialization, and sea level pressure (*SLP*) between experiments C0hci and C0h, and experiments C0hcimodis and C0hmodis. The results show that the initialization scheme has systematic impacts on all the variables. The larger *RMSE* of water vapor mixing ratio (*q*) between experiments C0hcimodis and C0hmodis than that between experiments C0hci and C0h also reflect the impact of the MODIS data that has been used to adjust the initial water vapor.

Figure 11 compares the RMSE between experiments C0h and C-6h, experiments C0hmodis and C-6h, as well as experiments C0hmodis and C0h. Comparing to the baseline experiment, the assimilation of the MODIS data causes large changes in water vapor and cloud ice from hours 0-6. Small changes are shown in

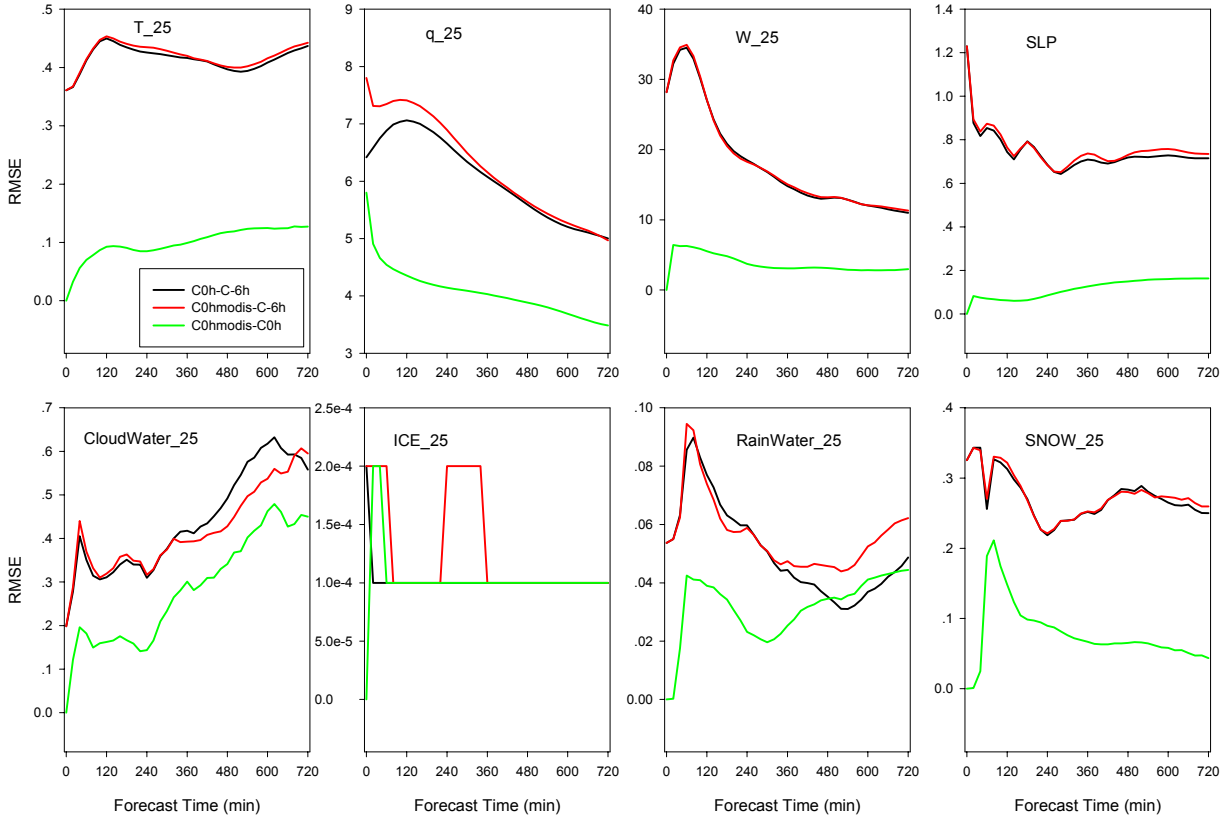

Figure 11. Same as Figure 10, but between the experiments C0h and C-6h, C0hmodis and C-6h, C0hmodis and C0h, at the 25th sigma level.

cloud water and rain water within the first 6 hours but increase afterwards. Comparing to the control run C0h, MODIS data introduces large differences to all the hydrometeor fields within the first hour. A slight change in vertical velocity can be seen in Figure 11. After 1 hour of simulation, the impacts are relatively small except the cloud water and rain water, which has larger differences later on.

6. CONCLUSIONS AND DISCUSSION

From the preliminary tests presented above and analysis of the results, following conclusions are obtained:

- The static cloud initialization scheme can produce cloud ice and cloud water at the initial time, which leads to a small improvement in precipitation forecast in the first 3 hours.
- Further improvement on initializing the temperature, mass and motion fields via a similar procedure, which strongly affect the cloud formation/deformation, is suggested.
- High-resolution MODIS data provides detailed information on clouds at least and appears to improve the cloud initialization scheme to start from a more accurate humidity field.

The above conclusions are drawn from preliminary tests at a single time period. More experiments are needed and the results will be presented at the conference.

***Acknowledgements*:** The study is supported by the University Partners Operational Support (UPOS) of the Department of Defense. Thanks Xiande Meng and Jeremy Krieger for data assistance. Thanks to UAF GINA facility and Kevin Eagle for MODIS assistance. The data used in this study were acquired as part of the NASA's Earth Science Enterprise. The algorithms were developed by the MODIS Science Teams. The data were processed by the MODIS Adaptive Processing System (MODAPS) and Goddard

Distributed Active Archive Center (DAAC), and are archived and distributed by the Goddard DAAC.

REFERENCES

Chen, F., and J. Dudhia, 2001: Coupling an advanced land surface hydrology model with the Penn State/NCAR MM5 modeling system. Part I: Model description and implementation. *Mon. Wea. Rev.*, **129**, 569-585.

Colle, B. A., K. J. Westrick, and C. F. Mass, 1999: Evaluation of MM5 and Eta-10 precipitation forecasts over the Pacific Northwest during the cool season. *Weather and Forecasting*, **14**, 137-154.

Dudhia, J., 1989: Numerical study of convection observed during the winter monsoon experiment using a mesoscale two-dimensional model. *J. Atmos. Sci.*, **46**, 3077-3107.

Fan, X., and J. S. Tilley, 2002: The impact of ssimilating satellite-derived humidity on MM5 forecasts. *15th Conference on Numerical Weather Prediction*, AMS, San Antonio, TX.

Grell, G. A., J. Dudhia, and D. R. Stauffer, 1994: A description of the Fifth-Generation Penn State/NCAR Mesoscale Model (MM5). NCAR/TN-389+IA, National Center for Atmospheric Research, CO, USA.

Lorenz, E. N., 1963: Deterministic nonperiodic flow. *J. Atmos. Sci.*, **20**, 130-141.

Mesinger, F., 1996: Improvements in quantitative precipitation forecasts with the Eta regional model at the National Centers for Environmental Prediction: The 48-km upgrade. *Bull. Amer. Meteor. Soc.*, **77**, 2637-2649.

Reisner, J., R. M. Rasmussen, and R. T. Bruintjes, 1998: Explicit forecasting of supercooled liquid water in winter storms using the MM5 mesoscale model. *Q. J. R. Meteorol. Soc.*, **124**, 1071-1107.

Wilks, D., 1995: Statistical *methods in the atmospheric sciences: An introduction*. Academic Press, 467 pp.